Gene expression remodeling, poly(A) tail regulation and alternative splicing define transcriptomic responses to microplastic exposure in the liverwort Riccia fluitans

Lukasz Paukszto

lukasz.paukszto@uwm.edu.pl

University of Warmia and Mazury in Olsztyn

Mateusz Mazdziarz

University of Warmia and Mazury in Olsztyn

Aleksandra Weiss

University of Warmia and Mazury in Olsztyn

Oskar Brzostek

University of Warmia and Mazury in Olsztyn

Joanna Szablińska

University of Warmia and Mazury in Olsztyn

Jarosław Calka

University of Warmia and Mazury in Olsztyn

Katarzyna Głowacka

University of Warmia and Mazury in Olsztyn

Paweł Sulima

University of Warmia and Mazury in Olsztyn

Katarzyna Krawczyk

University of Warmia and Mazury in Olsztyn

Research Article

Keywords:

Posted Date: May 31st, 2026

DOI: https://doi.org/10.21203/rs.3.rs-9846230/v1

Additional Declarations: No competing interests reported.

Abstract

Although micro- and nanoplastics (MNPs) are new environmental pollutants that are becoming more and more important for plant biology, little is known about how they affect early-diverging terrestrial plants molecularly. Using nanopore sequencing, we investigated the transcriptome responses of the liverwort *Riccia fluitans* to different concentrations of PET-derived MNPs. Exposure to the high dose triggered extensive transcriptome reprogramming, as reflected by pronounced differential gene expression, widespread poly(A) tail shortening, and alternative splicing changes. Genes associated with photosynthesis were mostly downregulated with shortened poly(A) tails, indicating disturbed translational control and mRNA stability. Stress pathways were strongly induced, especially in response to oxidative and abiotic stress. Alternative splicing analyses identified significant isoform switching in defense-related genes such as CAL3 and PAPR independent of overall expression changes. Our findings suggest that nanoplastics are strong abiotic stressors eliciting coordinated transcriptional and post-transcriptional regulation in *R. fluitans*. This study emphasizes conserved regulatory pathways across terrestrial plants and offers the first comprehensive long-read transcriptome analysis of MNP-induced stress responses in liverworts.

Introduction

The production of plastic is one of the leading contributors to environmental degradation that leaves a significant and lasting impact on the natural environment. Currently, approximately 79% of plastics is being accumulated in landfills, about 12% of plastic waste has been burned and only 9% has been recycled[1]. The mismanagement of plastics and its impact on the entire ecosystem is a reason for increasing safety concerns[2].

Microplastics and nanoplastics (MNPs), which are small particles of synthetic materials, have brought the world's attention due to their potential influence on the natural environment, aquatic habitats and human health. The main sources of MNPs are high-density polyethylene (HDPE), polyethylene terephthalate (PET), low-density polyethylene (LDPE)[3], as well as other types of polymers such as: polyethene (PE), polypropylene (PP), and polystyrene (PS)[4], out of which PET and PE are polymers with longer degradation period that contribute to the accumulation of microplastic particles in the ecosystem[5]. Micro and nanoplastics can also be distinguished based on their size. Most authors agree that microplastics are defined as particles ≤ 5 mm in size[4,6–8]. However, ter Halle and Ghiglione[6], citing data from the European Chemicals Agency (ECHA), provide a more detailed definition, describing microplastics as particles ranging from 100 nm to 5 mm. In contrast, the definition of nanoplastics varies considerably across sources. Some of them characterize NPs as either between 1 nm and 1 µm, 1 to < 100 nm or particles of size < 1µm [6,7,9].

According to Ashrafy et al.[4], MNPs can also be divided into two different categories based on their source of origin: primary, where the size of particles is specified during the production process, and

secondary microplastics, created from synthetic fabrics and macroplastic decomposition due to UV exposure. While Agboola and Benson[10] largely agree on this characterization, stating that primary MNPs come from direct production of plastic and secondary MNPs originate from the physical and chemical fragmentation of larger plastics, they emphasize the environmental harm of microplastics of both sources. Both micro- and nanoplastics enter the soil through wastewater treatment effluents, mulching, the use of organic fertilizers and daily human activity[11], which raises legitimate concerns regarding the health of animals and humans. For example, MNPs have been found in various aquatic taxa, such as fish, shrimp, turtles, bivalves, zooplankton and whales[8]. It has also been found in human lungs in the form of 250μm microfibers[9].

Given that nanoplastics are usually derived from the fragmentation of microplastics, they cause the same threat and the low rate of their degradation may cause long-term effects on the entire ecosystem[8]. What is more, in light of the aforementioned environmental degradation, it is also important to consider their effects on plant life. In this context, it is crucial to differentiate between nanoplastics with positive and negative surface charges. It has been discovered by Sun et al.[12], who studied the accumulation of both types in maize leaves, that while both can accumulate in plants, positively charged plastics bond more effectively due to negatively charged cell walls.

For nanoplastics to bioaccumulate and undergo internal transport within plants, they must first penetrate plant-imposed size exclusion limits (SELs). That means that only nanoplastics of specific sizes can overcome natural plant tissue barriers. A common way of crossing such borders involves the absorption via roots of the plant, followed by upward apoplastic transport or via intracellular spaces with the transpiration stream to aerial parts of the plant[13,14]. Cell walls can be penetrated by the nanoparticles within the size range of 5–20 nm [15]. It is also possible for nanoplastics to be taken in through stomata and then later be translocated toward the roots[12]. That means that nanoplastics can be easily and effectively transferred and absorbed in different parts of the plant. On the other hand, though there is no conclusive evidence of macroplastics tissue penetration, MPs can adhere on the surface of leaves and roots, which limits the water and nutrients uptake[16,17]. It has also been proven that micro- and nanoplastics can be transferred from plant-fed insects (*Tenebrio molitor*) to mice and accumulate in the lungs, liver, intestines, brain, and kidneys, as well as in embryos[18]. The evidence demonstrated by Monikh et al.[19] shows that particles of polystyrene and PVC, absorbed by lettuce roots that translocated to leaves, were found in insect larvae (*Hermetia illucens*) and finally accumulated in fish liver (Rutilus rutilus), becoming incorporated into that trophic chain.

The bioaccumulation of NPs and exposure to MPs in plants can have a direct toxic effect on their biochemical metabolism. A typical reaction to abiotic stress in plants, in this case exposure to plastic, is an accumulation of reactive oxygen species (ROS). The buildup of ROS in plant tissues causes biochemical imbalance and disrupts homeostasis, which triggers the activation of antioxidant response[17]. Oxidative response leads to growth reduction, increased lipid peroxidation, hydrogen peroxide accumulation, decreased photosynthesis efficiency and cytotoxic and genotoxic effects[20], that

eventually impacts the quality and quantity of accessible food[17]. It has been proven that when compared to the exposition to MPs, the absorption of different concentrations of small and positively charged NPs lead to a stronger oxidative response in different organisms, including plants[20,21].

Bioaccumulative potential and toxicity of plastic on plants depend on several factors, such as the polymer type, plant type, soil type, temperature, pH or UV radiation[22,23]. Non-biodegradable plastics easily absorb toxic chemicals[24], e.g. polyethylene (PE) increased the concentrations of Cd^{2+} in lettuce leaves by 25%[25]. Biodegradable polymers exhibit decreased risk of long-term bioaccumulation due to their accelerated degradation[22], the full decomposition is greatly dependent on aforementioned factors. Jansen et al.[23] raised concerns about reduced persistence of biodegradable polymers in the environment. Furthermore, the study conducted by Lei et al. (2019) suggests that microplastic toxicity is determined primarily by particle size rather than polymer composition.

As mentioned before, the micro- and nanoplastic prevalence is especially harmful for aquatic and soil biota. Among these organisms, bryophytes - mosses, hornworts and liverworts - are particularly vulnerable. Bryophytes not only enhance biodiversity, but also break down organic matter to recycle nutrients into the soil and serve as effective bioindicators[26]. This study centers on liverworts, emphasizing the necessity of a more comprehensive assessment of micro- and nanoplastic impacts on these organisms.

Liverworts, as members of bryophytes, represent one of the earliest-diverging lineages of land plants and display distinctive genomic evolutionary traits[27]. They usually have small, stable genomes that exhibit low variability in size and number of chromosomes, which is possible due to low duplication rate, low transposon activity and minimal chromosomal rearrangements. Despite that, liverworts demonstrate clear genomic diversity[28], which is likely due to its colonization of diverse worldwide habitats[27]. One of the examples of such a widespread and diverse genus of thalloid liverworts is *Riccia L.* and *Riccia fluitans* is its representative species[29].

Riccia fluitans is an amphibious plant that is able to survive in both water and land habitat and show different morphological traits, adjusted and dependent on the environment they inhabit. Land forms (LF) have more diverse and highly functional rhizoids and air pores, thicker cell walls and wax layer on epidermal walls when compared to water forms (WF) of the same species[30]. What is more, within days it can adapt to survive the change from water to land habitat, developing a thicker thallus as a form of defense mechanism against water loss[31]. Considering both water and land forms and its ability to adjust to environmental changes, *R. fluitans* is a great model for studying plants' responses to extensively changing environmental conditions, such as the presence of micro- and nanoplastic. Moreover, Althoff and Zachgo[32] have proven that it is also possible to genetically modify *R. fluitans*, which allows for a better analysis of its adaptive mechanisms.

Genetically, while analysing the land-water transition and differences in gene expression of both forms, *R.fluitans* demonstrated a robust transcriptional response with 45 down- and upregulated genes. Between the two forms there were noticeable differences in polyadenylation signals[31]. Polyadenylation is a process occurring in most eukaryotic organisms, where the long chain of adenine nucleotides is added to the 3' end of newly-synthesized mRNA, creating a poly(A) tail[33]. Poly(A) tails are fundamentally involved in translation enhancement, providing the stability of mRNA[34,35]. The length of these tails, which depends on the species and development stage, contributes significantly to that stability[35]. The elongated poly(A) tails observed in the transcripts of WF, which as previously stated are connected to the modulation of mRNA stability, indicate the existence of a defense mechanism to water stress[31].

Another crucial mechanism that ensures that plants adapt to changes in the environment is alternative splicing (AS) of pre-mRNAs. This posttranscriptional regulatory mechanism is essential during the formation of proteins, ensuring their functional complexity in eukaryotes[36]. Alternative splicing is a process where two or more mRNA forms are created from the same pre-mRNA thanks to different split sites. This in turn increases the diversity of the transcriptome and proteome, which affects the development of plants and impacts their main biological processes such as photosynthesis or flowering[37]. Molecular and genetic analysis show that AS is a key mechanism determining early developmental processes, germination, and maturing of seeds as well as seed dormancy[38]. About 60% of genes in the higher model plant *Arabidopsis thaliana* undergo AS[39]. What is more, AS takes part in modulating gene expression and most importantly, in regulating response to abiotic stresses[40] by targeting the abscisic acid (ABA) pathway[41].

Exposure to micro- and nanoplastics significantly affects gene expression across several different pathways in plants. According to Sun et al.[12], nanoplastic treatment of *A. thaliana* increased the expression of genes involved in the synthesis of flavonoids and compounds containing anthocyanin, both of which contribute to plant stress responses. Additionally, positively charged NPs caused the upregulation of genes associated with GO terms related to growth, survival and photosynthesis in *A. thaliana* shoots and increased the expression of peroxidases in its roots. Similarly, research on *A.thaliana* conducted by Dainelli et al.[42] shows the plastic-induced repression of ABA-response genes, upregulation of genes in xenobiotic detoxification and activation of many different stress-related transcripts, such as heat-shock proteins. Finally, the RNA-seq analysis by Martín et al.[43] who examined in vitro *Zea mays* seedlings treated with MPs, proved the significant changes in gene expression connected with stress-responses and metabolism, for example alteration of several sugar-transporter genes.

In this study, we analyze the impact of different doses of micro- and nanoplastic particles on *Riccia fluitans*, a species belonging to liverworts (*Marchantiopsida*). The aim of this study was to assess the effect of low and high doses of nanoplastic using differential expression and alternative splicing analyses and the assessment of differences in poly(A) tails between test samples.

Materials and Methods

PET nanoparticle preparation

A one-gram sample of polyester particles was mixed with 10 mL of concentrated trifluoroacetic acid (TFA, 90% v/v) at 50°C. For roughly two hours, the mixture was stirred vigorously and continuously until the polymer was completely dissolved. The solution that came out of it was then left alone overnight. To encourage the precipitation of the particulate material, 10 mL of a diluted aqueous TFA solution (20% v/v) was added to the main solution in small amounts while swirling it constantly. After being swirled for two hours, the blended liquid was left to sit overnight. Using centrifugation at 2500g for one hour, the sediment was separated from the supernatant. The pellet was then resuspended in 100 mL of a sodium dodecyl sulfate (SDS, 0.5% w/v) solution and agitated vigorously. It was then sonicated with a Vibra Cell™ VCX 600 (Sonics & Materials Inc.). After the procedure, the suspension was left to settle in a graduated cylinder for an hour without being disturbed. This made it easier for the bigger particles to separate by gravity. The upper liquid phase (50 mL) containing the nanoparticle suspension, called NanoPET, was carefully taken out so it could be used later. This NanoPET formulation has a longer shelf life and can be dried as needed.

Vegetative material, RNA isolation, and cDNA sequencing

Plants were cultivated in vitro, adhering to the methodology outlined in our prior publications[31]. Subsequent to this duration, the plants were subjected for two weeks to a suspension comprising plant material, RNA extraction, and cDNA sequencing. Subsequent to this duration, the plants were subjected for two weeks to a suspension containing nanoplastic particles at doses of 0.1 mg/L (LOW) and 10 mg/L (HIGH). The control group (CTR) was subjected to flooding without the presence of nanoplastic. After a fortnight, the plants were harvested, and their thalli were pulverized in a mortar with liquid nitrogen. Total RNA was subsequently extracted utilizing the Qiagen RNeasy Plant Mini Kit, adhering to the manufacturer's guidelines. The concentration of RNA was evaluated utilizing the QubitTM RNA HS Assay Kit and a Qubit fluorometer. Sequencing libraries for nanopore sequencing were constructed utilizing the PCR-cDNA Barcoding Kit SQK-PCB 111.24, employing 300 ng of total RNA per sample. The methodology comprised the subsequent steps: cDNA-RT adapter ligation, adapter digestion, reverse transcription, strand swapping, barcode incorporation, PCR utilizing rapid attachment primers, and the attachment of fast sequencing adapters. Library constructs were introduced into pre-primed MinION Flow Cell R 10.4.1 and sequenced using the MinION sequencing machine.

Scanning microscopy

The suspension of plastic particles was placed on formvar/carbon supported copper grids (Sigma-Aldrich) and left to dry at room temperature. Samples were analyzed with transmission electron

microscopy (TEM, JEOL JEM-1400; JEOL, Japan) at 80kV. Images were captured using a MORADA Olympus Soft Imaging Solutions digital camera.

Transcriptome profiling in Riccia fluitans.

Raw nanopore current data (POD5files) were basecalled using dorado v.0.8.1 (Oxford Nanopore Technologies)[44]. Basecalling was performed using the super-accurate (SUP) model. Reads were filtered to a minimum Q-score of 7. The resulting unaligned BAM files were converted to FASTQ format using bedtools v.2.30.0[45]. The FASTQ data were later aligned to the *R. fluitans* genome (GCA_043381455.1) with minimap2 v.2.27[46] with the -ax splice parameter. The analysis was carried out for two different microplastic doses, simultaneously. The gene expression profiles generated by the long-read sequencing approach were also assessed using StringTie v.3.0.0[47], GffRead v.0.12.7[48], featureCounts v.2.0.6[49], and DESeq2 v.1.42.0[50] R library. The statistical significance of differentially expressed genes was assessed using the following parameters: p.adjusted value < 0.05 and absolute log2FoldChange (log2FC) > 1. To categorize the genes into both groups, all genes were subjected to Blastp v.2.9.0[51] analysis (identity > 40% and coverage > 80%) against reference sequences from *Marchantia polymorpha* and *Arabidopsis thaliana* to identify potential homologs. Due to the use of dual references for annotating coding sequences, gene names from *Arabidopsis thaliana* were adopted, as it is a more comprehensively characterized model organism. In contrast, homology results against *Marchantia polymorpha* were more complete; however, many alignments exhibited an unclassified character. The homology Blastp method was also rerun for notable genes in the alternative splicing and polyA tails sections. Next, sequences were scanned by PLEK v.1.2[52] to confirm coding/noncoding potential. Based on those categories, notable genes were designated as differentially protein-coding genes (DEGs) and differentially long non-coding RNAs (DELs). The relationships among DEGs and DELs were assessed by co-expression analysis. Pairs of DEGs and DELs exhibiting similar transcriptome profiles were identified using Spearman correlation coefficient ($r > 0.99$, $p < 0.05$). Visualizations were generated using ggplot2[53] v.3.4.4 and circlize[54] v.0.4.15 packages in R Bioconductor v.3.18.

Analysis of PolyA tails

Secondary basecalling was performed using the 'sup' model, while the --reference flag (with the transcriptome being utilized as a reference) and the --estimate-poly-a flag were enabled. Variations in polyA tail lengths were examined using TAILcaller v.0.2.0[55]. For gene-level analysis, genes with fewer than 10 polyA tails were excluded. Genes were categorized as differentially polyadenylated genes (DPGs) when significant differences in polyadenylation were detected. Tail lengths were recorded, contingent upon achieving an adjusted p-value of less than 0.05. Based on the log2FC of polyA lengths, DPGs were classified as 'Collapsed' if the value was found to be less than 0, whereas they were categorized as 'Expansion' if the value was greater than 0.

Alternative splicing analysis

Transcript reconstruction and alternative splicing (AS) event detection were performed using ESPRESSO v. 1.6.0[56]. Using long-read cDNA Nanopore data, ESPRESSO generated a comprehensive transcriptome annotation incorporating novel isoforms and splice junctions. Differential alternative splicing (DAS) analysis was done using rMATS-long[57], which is made specifically for long-read RNA-seq data. Aligned BAM files from biological replicates were processed to identify and quantify AS events across experimental conditions. AS events were classified into categories: exon skipping, alternative 5' splice site, alternative 3' splice site, mutually exclusive exons, retained introns, alternative first, alternative last, alternative endpoints, combinatorial and complex. Statistical significance with FDR correction was determined using a significance threshold of 0.05. The selected DAS genes were compared between conditions according to isoform proportions measured in Counts Per Million (CPM) values. The internal rMATS-long script named visualize_isoforms.py[58], was used to visualize DAS genes.

Functional annotation

The DEGs, DPGs and DASes homologous with reference organisms were scanned to enrich Gene Ontology (GO) function annotations utilizing the g:Profiler v.0.2.2[59] R package with the gost function. To simplify and unify interpretation, only the *A.thaliana* database was used in gene functional assignment. Biological processes (BP), cellular components (CC), molecular functions (MF) and signaling pathways (KEGG) were designated as ontological signatures for the significant genes. An enrichment analysis with a false discovery rate (FDR) threshold of < 0.05 was conducted to uncover Gene Ontology (GO) and pathway annotations influenced by MNP-responsive target genes.

Data available

The Nanopore sequencing data used for genome assembly were deposited in the European Nucleotide Archive (ENA) database under BioProject PRJEB112774

Code availability

The guidelines for all bioinformatics tools employed in this study were strictly adhered. The software and code utilized are publicly available, with specific versions and parameters detailed in the Methods section. Our data compilation process did not involve any custom code.

Results

Morphological Characterization of Nanoplastic Particles

Nanoplastic particles in water were visualized (Fig. 1A). Plastic particles of varying sizes were observed in the sample, with dimensions ranging from nanoscale particles of approximately 2–5 nm to larger structures reaching up to 170 nm.

Expression profiling

As a result of sequencing 13 cDNA libraries using long-read technology, a total of 29 822 412 sequences were obtained. The average number of reads per sample was 2 485 201. After trimming and removal of potentially damaged or low-quality reads, a total of 26 941 698 reads were retained for downstream analyses. Before isolating nucleic acids from plants that were exposed to the stress factor, it was confirmed that MNP particles were present in the plant tissues (Fig. 1B). Subsequent mapping of sequences to the *Riccia fluitans* reference genome (GCA_043381455.1) and expression profiling under micro- and nanoplastic exposure revealed 21 014 transcriptionally active regions (TARs). The experiment aimed to investigate the effects of two microplastic concentrations, 0.1 mg/L (LOW) and 10 mg/L (HIGH), at multiple transcriptional levels, including overall gene expression profiles, poly(A) tail length variation, and alternative splicing patterns. Transcriptomic profile distribution with separation of the high-dose group from control samples was shown by the PCA analysis (Fig. 2A).

Differential expression analysis of *R. fluitans* under both MNP exposure levels demonstrated that only the high dose elicited significant alterations in global transcriptional profiles and in the proportion of transcriptional variants modulated by alternative splicing events. In contrast, both high and low-doses induced noticeable changes at the level of poly(A) tail length distribution. Among the 729 DE-TARs exhibiting differential expression in response to the high MNP dose, 459 genes were upregulated, while 270 genes were downregulated (Fig. 2B and C, E). The genes coding fatty acid desaturase A (*FADA)*, elongation factor family protein (*SVR3*) and OSBP (oxysterol binding protein)-related protein 4B (*ORP4B)* were in the group of top underexpressed targets after MNP high-dose exposition. However, genes coding endoplasmic reticulum oxidoreductins 2 (*ERO2*), peroxidase 2 (*PA2*), PP2C induced by AVRRPM1 (*PIA1*) showed the top overexpression in the treated group. Apart from already mentioned genes, there were also genes with higher expression differences between control and HIGH-dose groups, but overall they were considered unclassified proteins. Among all DE-TARs, 409 genes indicated homology to at least one of two reference organisms, and were defined as differentially expressed genes (DEGs) (Table S1). To identify homologs of protein-coding DEGs, the sequences were compared against two local protein databases - *Marchantia polymorpha* and *Arabidopsis thaliana*. All DEGs were found homologous to *Marchantia*, while 243 DEGs were matched to *Arabidopsis*. Within no-homology 320 DE-TARs, 158 transcripts had coding potential, and 162 were classified as DE-lncRNAs by PLEK software (Table S2). Expression profiles of both protein-coding genes and lncRNAs were correlated to identify potential regulatory gene-lncRNA pairs. Pearson’s correlation coefficient (> 0.99) indicated 216 positive and 92 negative trans-correlations between pairs of DE-lncRNAs (Fig. 2D).

Alternative Splicing Dynamics of CAL3 and PAPR Homologs Under High-Dose Nanoplastic Exposure

The analysis of alternative splicing (AS) events revealed differences in two genes encoding homologs of calmodulin 3 (*CAL3;* Fig. 3A, Table S3) and phosphoadenosine-phosphosulfate reductase (*PAPR;* Fig. 3B). Changes in alternative splicing patterns were observed exclusively under exposure to the high microplastic dose. In the case of the *calmodulin 3* gene, alternative splicing analysis revealed a predominance of the short isoform (*evm.model.chr1.2189*), which accounted for over 58.46% of all transcripts in control samples. However, in samples exposed to MNP, the relative abundance of this isoform decreased to 24.36%. The mean absolute expression levels (CPM) were 475.46 and 144.03 for the control and MNP-treated samples, respectively. This transcript represents a truncated form of the *CAL3* gene, which likely affects its coding potential and, consequently, may enhance its regulatory role in biological processes. The analysis identified five alternative variants of the PAPR gene. The results indicated that the second isoform (*MSTRG.15348.2*) of this gene exhibited markedly higher expression under high-dose MNP treatment. The mean proportion of this transcript accounted for 13.48% of all PAPR transcripts under control conditions, whereas in thalli exposed to MNP, its expression increased to over 56% of the total isoforms of this gene. The expression level, expressed in counts per million (CPM), reached 181.92 following high-dose microplastic exposure, compared with 31.79 under control conditions. The remaining isoforms did not display significant changes in their expression profiles. The transcript *MSTRG.15348.2* was characterized by skipping of exon 7, whereas the remaining four variants retained this exon in their gene structure.

Global and Gene-Specific Shifts in PolyA Tail Dynamics Under Nanoplastic Exposure

Estimated polyA lengths were derived from raw signals within the pod5 files (Fig. 4A), yielding data for 740,055 polyA tails with an overall mean length of 76. Across experimental groups, 510,804 polyA tails with a mean length of 78 were identified in the CTR group, 148,129 tails with a mean length of 73 were identified in the LOW group, and 81,122 tails with a mean length of 67 were identified in the HIGH group (Fig. 4B). Global differences in polyA tail lengths between groups were found to be significant ($p < 0.0001$), as were the pairwise comparisons of CTR vs. LOW ($p < 0.0001$) and CTR vs. HIGH ($p < 0.0001$) (Fig. 4B, 4C). At the gene level, 66 DPGs were detected in the CTR vs. HIGH comparison (Table S4), while 21 DPGs were identified in the CTR vs. LOW analysis (Table S5), with 11 DPGs being found common to both comparisons (Fig. 4B, 4D, 4E). In the CTR vs. HIGH comparison, 58 genes were classified as 'Collapsed' and 8 as 'Expansion'. Similarly, in the CTR vs. LOW comparison, 17 genes were categorized as 'Collapsed' and 4 as 'Expansion' (Fig. 4E). Notably, all 11 shared DPGs (comprising 10 'Collapsed' and 1 'Expansion' gene) were observed to exhibit a consistent profile across both concentrations; specifically, genes identified as 'Collapsed' in the CTR vs. HIGH comparison were also found to be 'Collapsed' in the CTR vs. LOW group. Genes exhibiting changes in poly(A) tail length between the low and high nanoplastik dose treatments also include those showing alterations in gene expression. This group encompasses genes encoding aldolase-type TIM barrel family protein (Arabidopsis thaliana TAIR database homolog: AT4G18360, log2FC = − 2.17, poly(A) tail length shortening = -40.822), pseudouridine synthase/archaeosine transglycosylase-like family protein (TAIR: AT4G14680; log2FC = − 1.68, poly(A) =

-58.01), 2Fe-2S ferredoxin-like superfamily protein (TAIR database: AT1G60950, log2FC = 2.53, poly(A) = -15.35), and calcium-sensing receptor (TAIR database: AT5G23060, log2FC = – 1.24, poly(A) = -54.85).

Functional annotation of DEGs and DPGs.

Using *A. thaliana* gene identifiers, enriched Gene Ontology (GO) analysis was performed, revealing the participation of DEGs in 32 biological processes, 16 molecular functions, and 17 cellular components (Table S6). Notably enriched GO terms included those related to photosynthesis, stress response, abiotic stimulus response, carbohydrate metabolism and biosynthesis, cell wall metabolism, and lipid metabolism. Among the genes exhibiting oxidoreductase activity (MF: GO:0016491), particular attention should be given to those associated with fatty acid metabolism, such as fatty acid hydroxylase suberfamily (*CER3*), fatty acid desaturase A (*FADA*), and fatty acid hydroxylase 1 (*FAH1*). Annotations within the BP category revealed several important processes regulated in the presence of microplastics, including “photosynthesis” (GO:0015979), “response to starvation” (GO:0042594), “starch metabolic process” (GO:0005982), “starch metabolic process” (GO:0005982), “response to oxidative stress” (GO:0006979) and “response to abiotic stimulus” (GO:0009628) (Fig. 5A). Nine of the eleven genes involved in photosynthesis that exhibited altered expression in response to high doses of MNP showed decreased expression, whereas only two genes encoding a Bestrophin-like protein and a 2Fe–2S ferredoxin-like superfamily protein were upregulated. Three of these photosynthesis biomarkers (*ZKT*, *VAR1*, *FED A*) and *SBPASE* were also involved in response to abiotic stimuli and starch metabolism, respectively (Fig. 5B). Genes whose expression is altered in response to microplastic exposure show patterns similar to those activated under starvation conditions, as indicated by the downregulation of seven marker genes (*ACDO1*, *ALN*, *APS3*, *ATH13*, *MIPS2*, *PES1* and *SQD1*) associated with responses to reduced nutrient availability and the upregulation of three of these genes (*PCK*, *PHT1* and *AT5G63190*). Among the upregulated genes is the gene encoding phosphoenolpyruvate carboxykinase 1 (*PCK*, logFC = 5.02), which represents one of the most strongly increasing genes in the liverwort thallus under stress induced by microplastic exposure.

Analysis of GO processes and KEGG pathways enrichment (Table S7) revealed significant alterations in polyA length in plant response to low- and high-dose of nanoplastics. Particularly prominent were processes associated with photosynthesis and abiotic stress resistance. The most significantly enriched GO biological process term was "photosynthesis, light harvesting in photosystem I" (GO:0009768), involving five homologues of Arabidopsis thaliana: AT2G05100 - *LHCB2.1*, AT3G27690 - *LHCB2.3*, AT1G08380 - *PSAO*, AT2G05070 - *LHCB2.2* and AT1G61520 - *LHCA3*. The broader "photosynthesis" term (GO:0015979) encompassed 10 genes, including components of light reactions (GO:0019684). Molecular functions included GO terms such as "chlorophyll binding" (GO:0016168) and GO cellular component "thylakoid" (GO:0009579). The "photosynthesis" pathway (KEGG:00195) featured five genes such as AT1G60950 - *FD2*, AT1G76100 - *PETE1*, AT4G04640 - *ATPC1*, AT1G08380 - *PSAO* and AT1G79040 - *PSBR* (Fig. 6). The FD2 gene indicated modification on polyA tail length and also on gene expression profile under high-dose MNP treatment. Other GO terms related to "Response to stress" (GO:0006950) involved 19 genes, linked to "response to abiotic stimulus" (GO:0009628). ROS-related

terms included "reactive oxygen species biosynthetic process" (GO:1903409) and "response to desiccation" (GO:0009269). No strongly enriched KEGG pathways specific to stress were identified ("Metabolic pathways" KEGG: 01100). These findings indicate nanoplastics-induced disruption of photosynthesis alongside activation of antioxidative mechanisms.

Discussion

Currently, few studies examine changes in gene expression in liverworts, such as the study by Tan et al.[60], and all exclude exposure to micro- and nanoplastics. This study investigates the in vitro cellular response to both high and low dosages of NPs. Overall, it has been found that the most crucial changes in gene expression were observed in samples with a high dosage of NPs in the following categories: photosynthesis, stress response, abiotic stimulus response, biosynthesis and metabolism of carbohydrates, cell wall metabolism, and metabolism of lipids.

Based on the functional enrichment analysis of genes, it was found that the expression of genes predominantly affecting photosynthesis has decreased in most cases (e.g. *ZKT, ACDO1, TAP38, PPD4, PPC2, FRO7, GUN5, SBPASE, VAR1*). The down-regulation of *FRO7*, a ferric reduction oxidase 7, responsible for Fe uptake in chloroplasts, causes acute chlorosis in plants grown in iron-deficient conditions[61]. A down-regulation of *TAP38* due to intense light exposure results in the lack of thylakoid-associated phosphatase, which in normal conditions removes phosphates from LHCII and therefore leads to LHCII hyperphosphorylation. This results in photoinhibition and impairment of the photosynthesis process[62,63]. Another example of an environmental stress factor affecting the activity of photosynthesis related genes is the prelonged period of drought, which down-regulates *GUN5*. It encodes CHLH - a H-subunit of Mg-chelatase, that takes part in the transport of Mg to protoporphyrin IX, an important role in the chlorophyll biosynthesis[64,65]. Interestingly, two genes were found to be significantly up-regulated: *FED A* and *VCCN1* (TAIR: *AT3G61320*). It is also noteworthy that transcripts of the *FED A* gene, despite showing clear overexpression under high MNP exposure, exhibited a significant shortening of poly(A) tail lengths. There is evidence that genes characterized by shortened poly(A) tails may also display a tendency toward attenuated expression, for example under drought stress[66]. The authors of this study demonstrate that during phosphorus deficiency and cold temperature (4°C), the *FED A* up-regulation is associated with changes in Fe management and photosynthetic energy demand due to altered metabolism and stress conditions. Simultaneously, the increased activity of *VCNN1* is connected with activation of photoprotective mechanisms, through proton motive force (PMF) fine-tuning, during rapid fluctuations in light intensity[67].

While describing the influence of stress-factors on photosynthesis in plants, it is worth mentioning that the shortening of poliA tails was observed in transcripts in which genes were mainly connected with photosynthetic functions. For the low concentration of nanoplastics, the downregulation occurred for genes like PRK or RCA. PRK encodes a phosphoribulokinase, which is essential in Calvin-Benson-Bassham cycle during photosynthesis, has been found to be downregulated under phosphate

deficiency[68,69]. The expression of RCA, that catalyses the activation of Rubisco, which is an enzyme involved in the assimilation of atmospheric CO_2 and photorespiratory carbon oxidation, has been found to be downregulated by jasmonates, which can mediate plants' reaction to abiotic and biotic stresses[70,71]. For the high concentration of nanoplastic, the expression was reduced in genes such as LHCB2.3 or PSBR. LHCB2.3 is a light-harvesting component in the thylakoid membrane, which is downregulated under low CO_2[72] and under cold stress in *Arabidopsis*[73]. The expression of PSBR, which encodes the PsbR subunit of photosystem II essential in photosynthesis, is reduced under drought stress[74,75].

There is a clear parallel between an impairment of gene expression and the activation of defense mechanisms when photosynthesis occurs in plants, which is similar when comparing micro/nanoplastic intrusion and the exposure to other external stress factors. This in turn suggests that micro/nanoplastic in plants does have a significant influence on photosynthesis, which is a key process for plants development[76]. Similar conclusion can be found in the study by Xu[77], which shows that the exposure to nanoplastic in rice leads to the decrease in gene expression connected to chlorophyll biosynthesis, photosynthesis and carbon metabolism.

In the stress response category connected to MNPs influence on plants, there was a notable upregulation of peroxidase family genes, namely *PRX25* (AT2G41480), *PRX52* (AT5G05340), *PRX71* (AT5G64120) and *PA2* (AT5G06720). Class III heme peroxidases are responsible for a heightened response related to abiotic stress exposure in plants, which involve oxidation of various substrates in the presence of H_2O_2 and ROS production[78]. The research by Eljebbawi et al.[79], studied the expression of class III peroxidase (CIII Prxs) genes in *A.thaliana* populations under stress-induced conditions. They found that under specific stresses, some CIII Prxs were upregulated. More specifically, the increased activity of PRX25, was observed in heat-elevated and salt conditions, the PRX52 under salt stress and PA2 under heat stress. PRX71 showed increased activity under all of the above-mentioned stress factors, which is particularly interesting given the highest increase in expression in the stress response category ($log_2FC = 5,2$) in response to NPs observed in this study. What is more, multiple other genes, all of which display the increased response to NPs in this study, were proved to exhibit upregulation associated with biotic and abiotic stresses. For instance, RD26 mediates the response to drought[80], AOX1A in *A.thaliana* shows enhanced activity under stresses like chilling, high salt or limited nutrients[81] and MPK4 which, when exposed to pathogens, regulates gene expression that activate plant's defense mechanisms [82,83].

Extensive overexpression of genes, with proven significant contribution in stress responses, results in the activation of several defence pathways in land plants. PER52 coding peroxidase 52, has a role in lignin biosynthesis, and the suppression of its production impacts the lignin composition of stem interfascicular fibres[84]. Peroxidase 71 coded by PER71 has a key role in responses to cell wall damages and exhibits overexpression as a reaction to cell wall integrity impairment[85]. Simultainously, increased expression of AOX1A improves UV-B tolerance and activates ROS defense systems in response to UV-

B[86]. Upregulation of identical genes demonstrated in our study suggests similarly strong defence reactions to NPs in liverworts.

It would appear that not only do nanoplastics induce particular stress response mechanisms, but also impact some reactions to abiotic stimuli in plants by either up- (e.g. RBOH F, NRT1.1, EXL2) or downregulation of genes (like CAO or CESA1). According to the research by Ma et al.[87], where they analyzed the influence of salt stress on two variants of *A.thaliana*, wild type and with mutated RBOH F gene, they found that the upregulation of RBOH F producing NADPH oxidase takes part in regulating Na^+/K^+ homeostasis by ROS generation. Therefore, upregulation of this gene by NPs suggests a strong reaction to stimulus, which could trigger regulation of ion balance in liverworts. Meanwhile, it has been proven that low levels of nitrite in the stem can upregulate NRT1.1, which promotes the opening of stomata in guard cells by nitrate induced depolarization[88,89]. Upregulation of NRT1.1 induced by NPs suggest that the blockage of nutrients to some parts of the plant could trigger stress driven stomatal movement. Schröder et al.[90] demonstrate upregulation of EXL2 during extended night periods and upon C deficiency (hypoxia stress), which leads to similar conclusions connected with NPs nutrient blockage, but this time evoking reactions to C starvation. What is more, the downregulation of chlorophyll b synthesizing gene CAO in wild type *A.thaliana*, which is caused by plants' light acclimation to high-light conditions, reduces the energy transfer rate, alters pigmentation and is a cause for visible photodamage[91,92]. This suggests that downregulation caused by NPs could cause a similar effect, related to impairment of basic functional mechanisms of land plants.

The NP-induced changes in the expression of genes involved in the biosynthesis and metabolism of carbohydrates, indicate just as strongly that there have been some major shifts in plant's metabolic priorities. For instance, a significantly upregulated gene SUS3, particularly expressed in guard cells, codes a sucrose-cleaving and synthesizing enzyme that provides UDP-glucose and fructose for many metabolic pathways. Starch production and carbon flux in guard cells causes turgor changes and stoma cell movements[93]. As previously stated, other genes like e.g. NRT1.1, that causes stomata opening during stress-induced conditions, are significantly upregulated as well. This suggests a higher need for nutrients in stoma cells during stress conditions caused by nanoplastics. What is more, Yang et al.[94] confirmed increased activity of SUS3 in the roots during drought stress conditions. Additionally, other genes that regulate plant nutrients content have been found to be upregulated by NPs. Hexokinase-1 encoding HXK1 increases the phosphorylation of glucose and regulates sugar pool size during drought and osmotic stress conditions [95]. PFK3 gene promotes glycolytic flux and ATP production in stress survival[96]. Finally, ICL along with MLS, both of which react to salt stress conditions, produce functionally linked enzymes that catalyse two consecutive steps in glyoxylate cycle, essential for ATP production[97–99]. Interestingly, a subset of genes in this category showed reduced expression, such as VTC2, GBSS1, ADG1, SDP1, APL2. Among these, a few representative examples can be noted, such as GBSS1, which is suppressed under salt stress conditions. This causes reduced biosynthesis of amylose, and therefore reduction of insoluble starch, which does not contribute under stress conditions, as it sequesters

available carbon from soluble sugars[100]. Another downregulated gene in response to stress is VTC2 coding GDP-L-galactose phosphorylase 1 required in ascorbate biosynthesis[101], which regulates stress signals in plants and when silenced during salt stress conditions, it shifts its mechanisms into a ROS-producing survival state[101,102].

There is a clear switch of focus in physiological functions connected with energy management in plants survival mode and carbohydrate biosynthesis, which is focused on its quick and efficient use. Similar gene expression results in NP-impacted plants suggest comparable behaviour, with active and naturally occurring endogenous adjustments of plant's mechanisms. Evidence for this has been reported in studies such as Xu[77]or Huang et al.[103], where both authors clearly demonstrate the impact that nanoplastics have on metabolism and biosynthesis of carbohydrates.

Consequently, changes in carbohydrates metabolism may also influence plants' cell wall structure. For instance, the enhanced expression of LSF1, connected with degradation of starch during low temperatures[104], could support the claim that plants have a strong need for readily available soluble sugars, i.a., for cell wall strengthening. Glucan phosphatase LSF1 promotes BAM1 in starch degradation[105,106], thus activating a β-amylase BAM1, which produces a possible source of sugars for callose priming, resulting in cell wall callose deposition[107,108]. Additionally, the functional enrichment analysis indicated that during nanoplastic-induced stress conditions, there was one more upregulated gene that may be connected with cell wall metabolism, specifically, a previously mentioned saccharose synthase-coding SUS3. However, there is no conclusive evidence that its activity greatly influences the cell wall during stress conditions. The study by Waititu et al.[109] suggests that the upregulation of SUS3 in draught-resistant line of maize seedling could be connected with a higher cellulose biosynthetic activity, thus taking part in maintaining cell wall integrity, yet it was solely concluded based on the gene ontology (GO) enrichment analysis and KEGG pathway analysis. Building upon this, the study by Yao et al.[110] strongly suggests that SUS3-produced enzyme should not be associated with cellulose synthesis, but other roles such as stomatal metabolism. There is also more evidence suggesting that during stress conditions, plants switch from energy-expensive anabolic to catabolic reactions, which could be used in processes like, e.g., cell wall strengthening. SBPASE enzymatic activity is critical in the accumulation of carbohydrates as well as modulating the carbon flux in the Calvin cycle by regenerating the RuBP (ribulose-1,5-bisphosphate), a molecule crucial for the proper functioning of photosynthesis[111,112]. Its NP-induced downregulation of this gene suggests an overall enhanced focus on catabolic-reactions in plant, which was also confirmed by Ding et al.[112], where they stated that stress-induced downregulation of SBPASE (MeJA and dark conditions), severely reduces the accumulation of starch and sucrose. What is more, the activity of ADG1 was reduced in leaves under drought conditions[113]. The GBSS1 producing granule-bound starch synthase I was downregulated under drought in rice spikelets[114] and during ABA/ethephon exposition in leaves[115]. The activity of all of the abovementioned genes in normal conditions is connected to starch biosynthesis[113–115] and all of them were found to be downregulated by nanoplastics.

Lastly, the functional enrichment analysis recognized only three different genes in the metabolism of lipids category: ICL, MLS, PMDH1. Two of them were upregulated when exposed to NPs, which were isocitrate lyase (ICL) and maltate synthase (MLS). Both of them code enzymes that catalyze consecutive steps in the glyoxylate cycle, taking part in lipid utilization and gluconeogenesis in plants[99,116] and as previously mentioned, it has been proven that ICL and MLS are significantly upregulated in rice when exposed to salt stress[98,99]. Though not only do they take part in energy production, but in the context of lipid metabolism, they take part in lipid utilization and gluconeogenesis in plants[116]. Finally, what further confirms plant's increased reliance on glycoxylate cycle, PMDH1, which codes one of the key enzymes in Krebs cycle (the TCA cycle) is reportedly downregulated when exposed to heat-shock[117] and has been found to be downregulated by nanoplastics as well.

Finally, it is necessary to mention the MNP-induced changes in transcript proportion in two genes, CAL3 and PAPR, that were observed as a result of the alternative splicing (AS) analysis. Although expression profiling has not shown an overall significant change in expression levels of these two genes, it has been found that the proportion of dominating transcript expression on a gene level has changed considerably in both cases. Several studies indicate that the activity of CAL3 contributes to the activation of defense mechanisms in plants connected with increased stress response. For example, CAL3 binds to the Ca^{2+} ions, that increase in concentration during heat stress (HS), creating Ca^{2+}/CaM complex modulating protein activity, and as a result, a variety of different physiological processes[118–120]. Such activity was observed in *Arabidopsis thaliana* and *Cucumis sativus* L.[119,120]. It has also been observed that in *Arabidopsis thaliana* root after 1h of Pb-induced stress, CAL3 showed increased activity that decreased in the later stages, which suggests that CAL3 serves as a probable Pb-stress indicator in early stages of plants' defense[121]. On the contrary, PAPR which is responsible for the reduction of activated SO_4^{2-}, a process important in stress response, has been well characterised in microorganisms such as *Escherichia coli* and yeast, but its occurrence in plants has only been documented in another bryophyte, *Physcomitrium patens*[122,123]. In the great majority of plants such as *A. thaliana*, it is adenosine-phosphosulfate reductase (APR) that takes part in the sulfate assimilation process [124,125]. What is more, based on the phylogenetic tree presented in Kopriva et al.[124], the amino acid sequence of putative *P. patens* PAPR is in closer relation with the ortholog in *Marchantia polymorpha*, than the APR in higher plants. In any case, the produced sulfite is later used as a donor for sulfation of compounds like peptides or hormones, which in their modulated form can be used during some important biological processes in plants, which include stress defense reactions dependent on sulfur-containing metabolites[126,127]. For instance, glutathione is a key sulphur-containing compound in stress reactions connected to chilling tolerance in maize or salinity response in rice[126]. It could very well be the case that the evident changes in PAPR transcript content are similarly connected to intense abiotic/biotic stress reactions.

All of the previously mentioned examples, as well as results acquired in this study suggest an important influence of nanoplastics on key metabolic processes in plants, including liverworts. The changes are mostly connected with stress-induced survival mode entering, related to accumulation of soluble sugars

which are easily accessible and fast to use, switching to mechanisms connected with utilisation of already accumulated macromolecular organic compounds, such as polysaccharides or lipids, and efficient energy storage and distribution.

Conclusion

This study concludes that nanoplastics markedly interfere with gene expression, poly(A) tail length, and alternative splicing in the liverwort Riccia fluitans, especially at elevated doses, reflecting known stress responses to abiotic factors such as drought, salinity, and nutrient scarcity. Elevated exposure to nanoplastics resulted in the downregulation of photosynthesis-related genes (e.g., FRO7, TAP38, GUN5), a reduction in poly(A) tail length of photosynthetic transcripts, and an upregulation of stress-response genes (e.g., PRX71, PRX52, AOX1A), thereby redirecting metabolism towards carbohydrate catabolism, lipid utilization through the glyoxylate cycle, and fortification of the cell wall. Alternative splicing modified transcript ratios in defense-related genes CAL3 and PAPR, indicating adaptive regulatory mechanisms preserved among bryophytes. These alterations demonstrate that nanoplastics serve as significant environmental stresses, triggering a survival mechanism that emphasizes fast energy mobilization rather than growth processes, aligning with observations in higher plants. Future study should investigate dose-response thresholds in bryophytes and the long-term ecological consequences, hence guiding measures to alleviate micro/nanoplastic pollution in aquatic ecosystems.

Declarations

Acknowledgements

This research was financially supported by the National Science Center, Poland [Grant No. 2023/07/X/NZ8/01263 (resources, methods establishment) and the statutory funding of University of Warmia and Mazury in Olsztyn (Grant No. 12.122.005-110 - *in vitro* cultures, sequencing procedure).

Authors and Affiliations

1. Department of Botany and Evolutionary Ecology, University of Warmia and Mazury in Olsztyn, Plac Łódzki 1, Olsztyn, 10-719, Poland
   Łukasz Paukszto, Katarzyna Krawczyk, Mateusz Maździarz, Oskar Brzostek
2. Department of Plant Physiology, Genetics and Biotechnology, University of Warmia and Mazury in Olsztyn, Oczapowskiego 1A, Olsztyn, 10-719, Poland
   Katarzyna Głowacka
3. Department of Genetics and Plant Pathophysiology, University of Warmia and Mazury in Olsztyn, Plac Łódzki 3, Olsztyn, 10-724, Poland
   Paweł Sulima & Joanna Szablińska

4. Department of Mathematical Methods of Computer Science, Institute of Computer Science, Faculty of Mathematics and Computer Science, University of Warmia and Mazury in Olsztyn, Słoneczna 54, 10-710 Olsztyn, Poland
Aleksandra Weiss
5. Department of Clinical Physiology, University of Warmia and Mazury in Olsztyn, Oczapowskiego 14, Olsztyn, 10-719, Poland
Jarosław Całka

Contributions

Ł.P., M.M. J.C and K.K. contributed to research design, K.K., K.G. and J.S-P. carried out laboratory analyses, Ł.P. and M.M. carried out bioinformatic analyses and visualized data, J.S-P. and K.K. collected samples, P.S. were responsible for *in vitro* cultures, Ł.P., A.W., O.B., M.M. and K.K. wrote the original draft. Ł.P. obtained funding. Ł.P. conceptualization. All authors revised and approved the final version of the manuscript.

Corresponding authors

Correspondence to Łukasz Paukszto - lukasz.paukszto@uwm.edu.pl

Ethics declarations

Competing interests

The authors declare no competing interests.

Additional information

Publisher's note Springer Nature remains neutral with regard to jurisdictional claims in published maps and institutional affiliations.

References

1. Geyer R, Jambeck JR, Law KL. Production, use, and fate of all plastics ever made. Sci Adv 3, (2017).
2. Aneja S, Kalakoti S, Parihar DS. Urgent Need of Plastic Waste Management: A Review. Res Rev Int J Multidisciplinary. 2024;9:114–24.
3. Hossain R, Islam MT, Ghose A, Sahajwalla V. Full circle: Challenges and prospects for plastic waste management in Australia to achieve circular economy. J Clean Prod 368, (2022).
4. Ashrafy A, et al. Microplastics Pollution: A Brief Review of Its Source and Abundance in Different Aquatic Ecosystems. J Hazard Mater Adv. 2023;9:100215.
5. Yang Y, et al. Plastic wastes (PWs) and microplastics (MPs) formation: Management, migration, and environmental impact. J Environ Chem Eng. 2024;12:112926.
6. ter Halle A, Ghiglione JF, Nanoplastics. A Complex, Polluting Terra Incognita. Environ Sci Technol. 2021;55:14466–9.
7. Koelmans AA, et al. Microplastics in freshwaters and drinking water: Critical review and assessment of data quality. Water Res. 2019;155:410–22.
8. Chen G, Feng Q, Wang J. Mini-review of microplastics in the atmosphere and their risks to humans. Sci Total Environ 703, (2020).
9. de Bruin CR, de Rijke E, van Wezel AP, Astefanei A. Methodologies to characterize, identify and quantify nano- and sub-micron sized plastics in relevant media for human exposure: a critical review. Environ Sci Adv. 2022;1:238–58.
10. Agboola OD, Benson NU. Physisorption and Chemisorption Mechanisms Influencing Micro (Nano) Plastics-Organic Chemical Contaminants Interactions: A Review. Front Environ Sci. 2021;9:678574.
11. Azeem I et al. Uptake and Accumulation of Nano/Microplastics in Plants: A Critical Review. Nanomaterials (Basel) 11, (2021).
12. Sun H, Lei C, Xu J, Li R. Foliar uptake and leaf-to-root translocation of nanoplastics with different coating charge in maize plants. J Hazard Mater 416, (2021).
13. Li L, et al. Effective uptake of submicrometre plastics by crop plants via a crack-entry mode. Nat Sustain. 2020;3:929–37.
14. Sahai H, Bueno MJM, del Mar Gómez-Ramos M, Fernández-Alba AR, Hernando MD. Quantification of nanoplastic uptake and distribution in the root, stem and leaves of the edible herb Lepidum sativum. Sci Total Environ 912, (2024).
15. Rai M, et al. Copper and copper nanoparticles: Role in management of insect-pests and pathogenic microbes. Nanotechnol Rev. 2018;7:303–15.

16. Urbina MA, Correa F, Aburto F, Ferrio JP. Adsorption of polyethylene microbeads and physiological effects on hydroponic maize. Sci Total Environ. 2020;741:140216.
17. Roy T, Dey TK, Jamal M. Microplastic/nanoplastic toxicity in plants: an imminent concern. *Environmental Monitoring and Assessment* 2022 195:1 195, 1–35 (2023).
18. Wang Y et al. From insects to mammals! Tissue accumulation and transgenerational transfer of micro/nano-plastics through the food chain. J Hazard Mater 480, (2024).
19. Abdolahpur Monikh F et al. Quantifying the trophic transfer of sub-micron plastics in an assembled food chain. Nano Today 46, (2022).
20. Ekner-Grzyb A, Duka A, Grzyb T, Lopes I. & Chmielowska-Bąk, J. Plants oxidative response to nanoplastic. Front Plant Sci 13, (2022).
21. Gonçalves JM, Bebianno MJ. Nanoplastics impact on marine biota: A review. Environ Pollut 273, (2021).
22. Boctor J et al. Microplastics and nanoplastics: fate, transport, and governance from agricultural soil to food webs and humans. Environ Sci Eur 37, (2025).
23. Jansen MAK et al. Plastics in the environment in the context of UV radiation, climate change and the Montreal Protocol: UNEP Environmental Effects Assessment Panel, Update 2023. *Photochemical & Photobiological Sciences* 2024 23:4 23, 629–650 (2024).
24. Palmer J, Herat S. Ecotoxicity of Microplastic Pollutants to Marine Organisms: a Systematic Review. Water Air Soil Pollut 232, (2021).
25. Wang F, Wang X, Song N. Polyethylene microplastics increase cadmium uptake in lettuce (Lactuca sativa L.) by altering the soil microenvironment. Sci Total Environ 784, (2021).
26. Sawangproh W. Microplastic contamination of bryophytes: A review on mechanisms and impacts. Heliyon. 2024;10:e36360.
27. Maul K, Gradstein SR, Quandt D, Kessler M. Temperature dependence of liverwort diversification reveals a cool origin and hot hotspots. Sci Rep 15, (2025).
28. Linde AM, et al. Genome Evolution in Plants: Complex Thalloid Liverworts (Marchantiopsida). Genome Biol Evol. 2023;15:evad014.
29. Cargill DC, Neal WC, Sharma I, Gueidan C. A preliminary molecular phylogeny of the genus Riccia L. (Ricciaceae) in Australia. Aust Syst Bot. 2016;29:197–217.
30. Althoff F, Wegner L, Ehlers K, Buschmann H, Zachgo S. Developmental Plasticity of the Amphibious Liverwort Riccia fluitans. Front Plant Sci. 2022;13:909327.
31. Maździarz M, et al. Epitranscriptome insights into Riccia fluitans L. (Marchantiophyta) aquatic transition using nanopore direct RNA sequencing. BMC Plant Biol. 2024;24:1–16.
32. Althoff F, Zachgo S. Transformation of Riccia fluitans, an Amphibious Liverwort Dynamically Responding to Environmental Changes. Int J Mol Sci. 2020;21:1–16.
33. Nicholson AL, Pasquinelli AE. Tales of Detailed Poly(A) Tails. Trends Cell Biol. 2019;29:191–200.

34. Lima SA, et al. Short poly(A) tails are a conserved feature of highly expressed genes. Nat Struct Mol Biol. 2017;24:1057–63.
35. Subtelny AO, Eichhorn SW, Chen GR, Sive H, Bartel DP. Poly(A)-tail profiling reveals an embryonic switch in translational control. Nature. 2014;508:66–71.
36. Reddy ASN, Marquez Y, Kalyna M, Barta A. Complexity of the alternative splicing landscape in plants. Plant Cell. 2013;25:3657–83.
37. Reddy AS. N. Alternative splicing of pre-messenger RNAs in plants in the genomic era. Annu Rev Plant Biol. 2007;58:267–94.
38. Szakonyi D, Duque P. Alternative splicing as a regulator of early plant development. Front Plant Sci. 2018;9:382146.
39. Carvalho RF, Feijão CV, Duque P. On the physiological significance of alternative splicing events in higher plants. *Protoplasma 250:3* 250, 639–650 (2013).
40. Staiger D, Brown JWS. Alternative Splicing at the Intersection of Biological Timing, Development, and Stress Responses. Plant Cell. 2013;25:3640–56.
41. Laloum T, Martín G, Duque P. Alternative Splicing Control of Abiotic Stress Responses. Trends Plant Sci. 2018;23:140–50.
42. Dainelli M et al. Coding and non-coding transcripts modulated by transparent and blue PET micro-nanoplastics in Arabidopsis thaliana. Plant Physiol Biochem 220, (2025).
43. Martín C, et al. Transcriptomic and physiological effects of polyethylene microplastics on Zea mays seedlings and their role as a vector for organic pollutants. Chemosphere. 2023;322:138167.
44. GitHub - nanoporetech/dorado. Oxford Nanopore's Basecaller · GitHub. https://github.com/nanoporetech/dorado
45. Quinlan AR, Hall IM. BEDTools: a flexible suite of utilities for comparing genomic features. Bioinformatics. 2010;26:841–2.
46. Li H. Minimap2: pairwise alignment for nucleotide sequences. Bioinformatics. 2018;34:3094–100.
47. Shumate A, Wong B, Pertea G, Pertea M. Improved transcriptome assembly using a hybrid of long and short reads with StringTie. PLoS Comput Biol. 2022;18:e1009730.
48. Pertea G, Pertea M, Stroehlein AGFF, Utilities. GffRead and GffCompare [version 2; peer review: 3 approved] report report report. https://doi.org/10.12688/f1000research.23297.1 (2020) doi:10.12688/f1000research.23297.1.
49. Liao Y, Smyth GK, Shi W. Sequence analysis featureCounts: an efficient general purpose program for assigning sequence reads to genomic features. 30, 923–30 (2014).
50. Love MI, Huber W, Anders S. Moderated estimation of fold change and dispersion for RNA-seq data with DESeq2. Genome Biol. 2014;15:550.
51. Camacho C et al. BLAST+: architecture and applications. https://doi.org/10.1186/1471-2105-10-421 (2009) doi:10.1186/1471-2105-10-421.

52. Li A, Zhang J, Zhou Z. PLEK: a tool for predicting long non-coding RNAs and messenger RNAs based on an improved k-mer scheme. BMC Bioinformatics. 2014;15:311.
53. Wickham H. Ggplot2: Elegant Graphics for Data Analysis. New York: Springer-; 2016.
54. GitHub - jokergoo/circlize. Circular visualization in R · GitHub. https://github.com/jokergoo/circlize
55. Maździarz M, Paukszto Ł, Sawicki J. TAILcaller: an R package for analyzing differences in poly(A) tail length for Oxford Nanopore RNA sequencing. Bioinf Adv 5, (2024).
56. Gao Y, et al. Robust discovery and quantification of transcript isoforms from error-prone long-read RNA-seq data. Sci Adv 9. 2023;ESPRESSO:eabq5072.
57. GitHub - Xinglab. /rMATS-long · GitHub. https://github.com/Xinglab/rMATS-long
58. rMATS-. long/src/rmats_long/visualize_isoforms.py at main · Xinglab/rMATS-long · GitHub. https://github.com/Xinglab/rMATS-long/blob/main/src/rmats_long/visualize_isoforms.py
59. Reimand J, et al. g:Profiler—a web server for functional interpretation of gene lists. Nucleic Acids Res. 2016;44:W83–9.
60. Tan QW et al. Cross-stress gene expression atlas of Marchantia polymorpha reveals the hierarchy and regulatory principles of abiotic stress responses. *Nature Communications 2023 14:1* 14, 1–19 (2023).
61. Jeong J et al. Chloroplast Fe(III) chelate reductase activity is essential for seedling viability under iron limiting conditions. *Proc. Natl. Acad. Sci. U. S. A.* 105, 10619–10624 (2008).
62. Rantala M, Lehtimäki N, Aro EM, Suorsa M. Downregulation of TAP38/PPH1 enables LHCII hyperphosphorylation in Arabidopsis mutant lacking LHCII docking site in PSI. FEBS Lett. 2016;590:787.
63. Serrano-Pérez E, et al. Transcriptomic and Metabolomic Response to High Light in the Charophyte Alga Klebsormidium nitens. Front Plant Sci. 2022;13:855243.
64. Mochizuki N, Brusslan JA, Larkin R, Nagatani A, Chory J. Arabidopsis genomes uncoupled 5 (GUN5) mutant reveals the involvement of MG-chelatase H subunit in plastid-to-nucleus signal transduction. *Proc. Natl. Acad. Sci. U. S. A.* 98, 2053–2058 (2001).
65. Phung TH, et al. Porphyrin Biosynthesis Control under Water Stress: Sustained Porphyrin Status Correlates with Drought Tolerance in Transgenic Rice. Plant Physiol. 2011;157:1746.
66. Gao X, et al. Transcriptome analysis provides new insights into plants responses under phosphate starvation in association with chilling stress. BMC Plant Biol. 2022;22:26.
67. Herdean A, et al. A voltage-dependent chloride channel fine-tunes photosynthesis in plants. Nat Commun. 2016;7:11654.
68. Yu A, et al. Photosynthetic Phosphoribulokinase Structures: Enzymatic Mechanisms and the Redox Regulation of the Calvin-Benson-Bassham Cycle. Plant Cell. 2020;32:1556.
69. Kang J, et al. Suppression of Photosynthetic Gene Expression in Roots Is Required for Sustained Root Growth under Phosphate Deficiency. Plant Physiol. 2014;165:1156–70.

70. Shan X, et al. The Role of Arabidopsis Rubisco Activase in Jasmonate-Induced Leaf Senescence. Plant Physiol. 2010;155:751.
71. Zhang J, et al. Identification of two bZIP transcription factors interacting with the promoter of soybean rubisco activase gene (GmRCAα). Front Plant Sci. 2016;7:186176.
72. Li Y, Xu J, Haq NU, Zhang H, Zhu XG. Was low CO2 a driving force of C4 evolution: Arabidopsis responses to long-term low CO2 stress. J Exp Bot. 2014;65:3657–67.
73. Stock J, et al. The transcription factor WRKY22 is required during cryo-stress acclimation in Arabidopsis shoot tips. J Exp Bot. 2020;71:4993.
74. Shaar-Moshe L, Hübner S, Peleg Z. Fatty acid profiles and their distribution patterns in microalgae: a comprehensive analysis of more than 2000 strains from the SAG culture collection. https://doi.org/10.1186/s12870-015-0493-6 (2011) doi:10.1186/s12870-015-0493-6.
75. Brenner WG, Schmülling T. Transcript profiling of cytokinin action in Arabidopsis roots and shoots discovers largely similar but also organ-specific responses. BMC Plant Biol. 2012;12:112.
76. Muhammad A, Photosynthesis. The Key Driver of Plant Growth and Development. J Clin Stud Med Case Rep. 2024;11:1–4.
77. Xu C. The Oryza sativa transcriptome responds spatiotemporally to polystyrene nanoplastic stress. Sci Total Environ 928, (2024).
78. Passardi F, Penel C, Dunand C. Performing the paradoxical: How plant peroxidases modify the cell wall. Trends Plant Sci. 2004;9:534–40.
79. Eljebbawi A, Savelli B, Libourel C, Estevez JM, Dunand C. Class III Peroxidases in Response to Multiple Abiotic Stresses in Arabidopsis thaliana Pyrenean Populations. Int J Mol Sci. 2022;23:3960.
80. Ye H, et al. RD26 mediates crosstalk between drought and brassinosteroid signalling pathways. Nat Commun. 2017;8:14573.
81. Feng H, et al. Expression and signal regulation of the alternative oxidase genes under abiotic stresses. Acta Biochim Biophys Sin (Shanghai). 2013;45:985–94.
82. Qiu JL, et al. Arabidopsis MAP kinase 4 regulates gene expression through transcription factor release in the nucleus. EMBO J. 2008;27:2214.
83. He WZ, et al. Transcriptomic profiling reveals the complex interaction between a bipartite begomovirus and a cucurbitaceous host plant. BMC Genomics. 2024;25:1–12.
84. Fernández-Pérez F, Pomar F, Pedreño MA, Novo-Uzal E. The suppression of AtPrx52 affects fibers but not xylem lignification in Arabidopsis by altering the proportion of syringyl units. Physiol Plant. 2015;154:395–406.
85. Raggi S, et al. The Arabidopsis Class III Peroxidase AtPRX71 Negatively Regulates Growth under Physiological Conditions and in Response to Cell Wall Damage. Plant Physiol. 2015;169:2513–25.
86. Garmash EV, Velegzhaninov IO, Ermolina KV, Rybak AV, Malyshev RV. Altered levels of AOX1a expression result in changes in metabolic pathways in Arabidopsis thaliana plants acclimated to low dose rates of ultraviolet B radiation. Plant Sci 291, (2020).

87. Ma L, et al. NADPH oxidase AtrbohD and AtrbohF function in ROS-dependent regulation of Na+/K+ homeostasis in Arabidopsis under salt stress. J Exp Bot. 2012;63:305–17.
88. Sakuraba Y, Chaganzhana, Mabuchi A, Iba K, Yanagisawa S. Enhanced NRT1.1/NPF6.3 expression in shoots improves growth under nitrogen deficiency stress in Arabidopsis. *Communications Biology* 2021 4:1 4, 1–14 (2021).
89. Guo FQ, Young J, Crawford NM. The Nitrate Transporter AtNRT1.1 (CHL1) Functions in Stomatal Opening and Contributes to Drought Susceptibility in Arabidopsis. Plant Cell. 2003;15:107–17.
90. Schröder F, Lisso J, Müssig C. Expression pattern and putative function of EXL1 and homologous genes in Arabidopsis. Plant Signal Behav. 2012;7:22–7.
91. Tanaka R, Tanaka A. Effects of chlorophyllide a oxygenase overexpression on light acclimation in Arabidopsis thaliana. Photosynth Res. 2005;85:327–40.
92. Sakuraba Y, Yokono M, Akimoto S, Tanaka R, Tanaka A. Deregulated chlorophyll b synthesis reduces the energy transfer rate between photosynthetic pigments and induces photodamage in Arabidopsis thaliana. Plant Cell Physiol. 2010;51:1055–65.
93. Piro L, Flütsch S, Santelia D. Arabidopsis Sucrose Synthase 3 (SUS3) regulates starch accumulation in guard cells at the end of day. Plant Signal Behav. 2023;18:2171614.
94. Yang Y et al. Root Physiological Traits and Transcriptome Analyses Reveal that Root Zone Water Retention Confers Drought Tolerance to Opisthopappus taihangensis. *Scientific Reports* 2020 10:1 10, 2627- (2020).
95. Wu R, et al. Hexokinase1: A glucose sensor involved in drought stress response and sugar metabolism depending on its kinase activity in strawberry. Front Plant Sci. 2023;14:1069830.
96. Fugate KK, Morin M, Eide JD, Lafta AM, Finger FL. Wounding causes rapid, intense upregulation of glycolytic and fermentative genes and enzymatic activities in harvested sugarbeet roots. *Scientific Reports 2025 15:1* 15, 21709- (2025).
97. Maruyama K, et al. Integrated Analysis of the Effects of Cold and Dehydration on Rice Metabolites, Phytohormones, and Gene Transcripts. Plant Physiol. 2014;164:1759.
98. Thanabut S, Sornplerng P, Buaboocha T. Ectopic expression of rice malate synthase in Arabidopsis revealed its roles in salt stress responses. J Plant Physiol 280, (2023).
99. Yuenyong W, Sirikantaramas S, Qu LJ, Buaboocha T. Isocitrate lyase plays important roles in plant salt tolerance. BMC Plant Biol. 2019;19:472.
100. Chen HJ, Chen JY, Wang SJ. Molecular regulation of starch accumulation in rice seedling leaves in response to salt stress. Acta Physiol Plant. 2008;30:135–42.
101. Kakan X, et al. Ascorbic acid modulation by ABI4 transcriptional repression of VTC2 in the salt tolerance of Arabidopsis. BMC Plant Biol. 2021;21:112.
102. Dowdle J, Ishikawa T, Gatzek S, Rolinski S, Smirnoff N. Two genes in Arabidopsis thaliana encoding GDP-L-galactose phosphorylase are required for ascorbate biosynthesis and seedling viability. Plant J. 2007;52:673–89.

103. Huang D, et al. Insights into growth-affecting effect of nanomaterials: Using metabolomics and transcriptomics to reveal the molecular mechanisms of cucumber leaves upon exposure to polystyrene nanoplastics (PSNPs). Sci Total Environ. 2023;866:161247.
104. Zhou H, et al. Dynamics of starch degradation and expression of related genes during chilling stress in grapevine. Hortic Adv. 2023;1:3.
105. Liu J, et al. The LIKE SEX FOUR 1–malate dehydrogenase complex functions as a scaffold to recruit β-amylase to promote starch degradation. Plant Cell. 2023;36:194.
106. Schreier TB, et al. LIKE SEX4 1 Acts as a β-Amylase-Binding Scaffold on Starch Granules during Starch Degradation. Plant Cell. 2019;31:2169.
107. Gamir J, et al. Starch degradation, abscisic acid and vesicular trafficking are important elements in callose priming by indole-3-carboxylic acid in response to Plectosphaerella cucumerina infection. Plant J. 2018;96:518–31.
108. Sanmartín N, et al. Role and mechanisms of callose priming in mycorrhiza-induced resistance. J Exp Bot. 2020;71:2769–81.
109. Waititu JK, et al. Transcriptome analysis of tolerant and susceptible maize genotypes reveals novel insights about the molecular mechanisms underlying drought responses in leaves. Int J Mol Sci. 2021;22:6980.
110. Yao D, Gonzales-Vigil E, Mansfield SD. Arabidopsis sucrose synthase localization indicates a primary role in sucrose translocation in phloem. J Exp Bot. 2019;71:1858.
111. Tamoi M, Nagaoka M, Miyagawa Y, Shigeoka S. Contribution of fructose-1,6-bisphosphatase and sedoheptulose-1,7-bisphosphatase to the photosynthetic rate and carbon flow in the Calvin cycle in transgenic plants. Plant Cell Physiol. 2006;47:380–90.
112. Ding F, Wang M, Zhang S. Sedoheptulose-1,7-Bisphosphatase is Involved in Methyl Jasmonate- and Dark-Induced Leaf Senescence in Tomato Plants. Int J Mol Sci. 2018;19:3673.
113. Egea I et al. The drought-tolerant Solanum pennellii regulates leaf water loss and induces genes involved in amino acid and ethylene/jasmonate metabolism under dehydration. *Scientific Reports 2018 8:1* 8, 2791- (2018).
114. Zhu G, Ye N, Yang J, Peng X, Zhang J. Regulation of expression of starch synthesis genes by ethylene and ABA in relation to the development of rice inferior and superior spikelets. J Exp Bot. 2011;62:3907.
115. Gonçalves LP, et al. Rootstock-induced molecular responses associated with drought tolerance in sweet orange as revealed by RNA-Seq. BMC Genomics. 2019;20:110.
116. Cornah JE, Germain V, Ward JL, Beale MH, Smith SM. Lipid utilization, gluconeogenesis, and seedling growth in Arabidopsis mutants lacking the glyoxylate cycle enzyme malate synthase. J Biol Chem. 2004;279:42916–23.
117. Wang L, et al. Differential physiological, transcriptomic and metabolomic responses of Arabidopsis leaves under prolonged warming and heat shock. BMC Plant Biol. 2020;20:86.

118. Liu S, et al. Calmodulins and calmodulin-like proteins-mediated plant organellar calcium signaling networks under abiotic stress. Crop J. 2024;12:1321–32.
119. Yu B, et al. Overexpression of CsCaM3 improves high temperature tolerance in cucumber. Front Plant Sci. 2018;9:304566.
120. Zhang W, et al. Molecular and genetic evidence for the key role of AtCaM3 in heat-shock signal transduction in Arabidopsis. Plant Physiol. 2009;149:1773–84.
121. Zheng S, Ren P, Zhai M, Li C, Chen Q. Identification of Genes Involved in Root Growth Inhibition Under Lead Stress by Transcriptome Profiling in Arabidopsis. Plant Mol Biol Rep. 2021;39:50–9.
122. Koprivova A, et al. Functional knockout of the adenosine 5’-phosphosulfate reductase gene in Physcomitrella patens revives an old route of sulfate assimilation. J Biol Chem. 2002;277:32195–201.
123. Kopriva S, Karvansara PR, Takahashi H. Adaptive modifications in plant sulfur metabolism over evolutionary time. J Exp Bot. 2024;75:4697–711.
124. Kopriva S, Fritzemeier K, Wiedemann G, Reski R. The Putative Moss 3'-Phosphoadenosine-5'-phosphosulfate Reductase Is a Novel Form of Adenosine-5'-phosphosulfate Reductase without an Iron-Sulfur Cluster. J Biol Chem. 2007;282:22930–8.
125. Stevenson CEM, Hughes RK, McManus MT, Lawson DM, Kopriva S. The X-ray crystal structure of APR-B, an atypical adenosine 5'-phosphosulfate reductase from Physcomitrella patens. FEBS Lett. 2013;587:3626–32.
126. Koprivova A, Kopriva S. Sulfur metabolism and its manipulation in crops. J Genet Genomics. 2016;43:623–9.
127. Kopriva S, Malagoli M, Takahashi H. Sulfur nutrition: impacts on plant development, metabolism, and stress responses. J Exp Bot. 2019;70:4069–73.

Figures

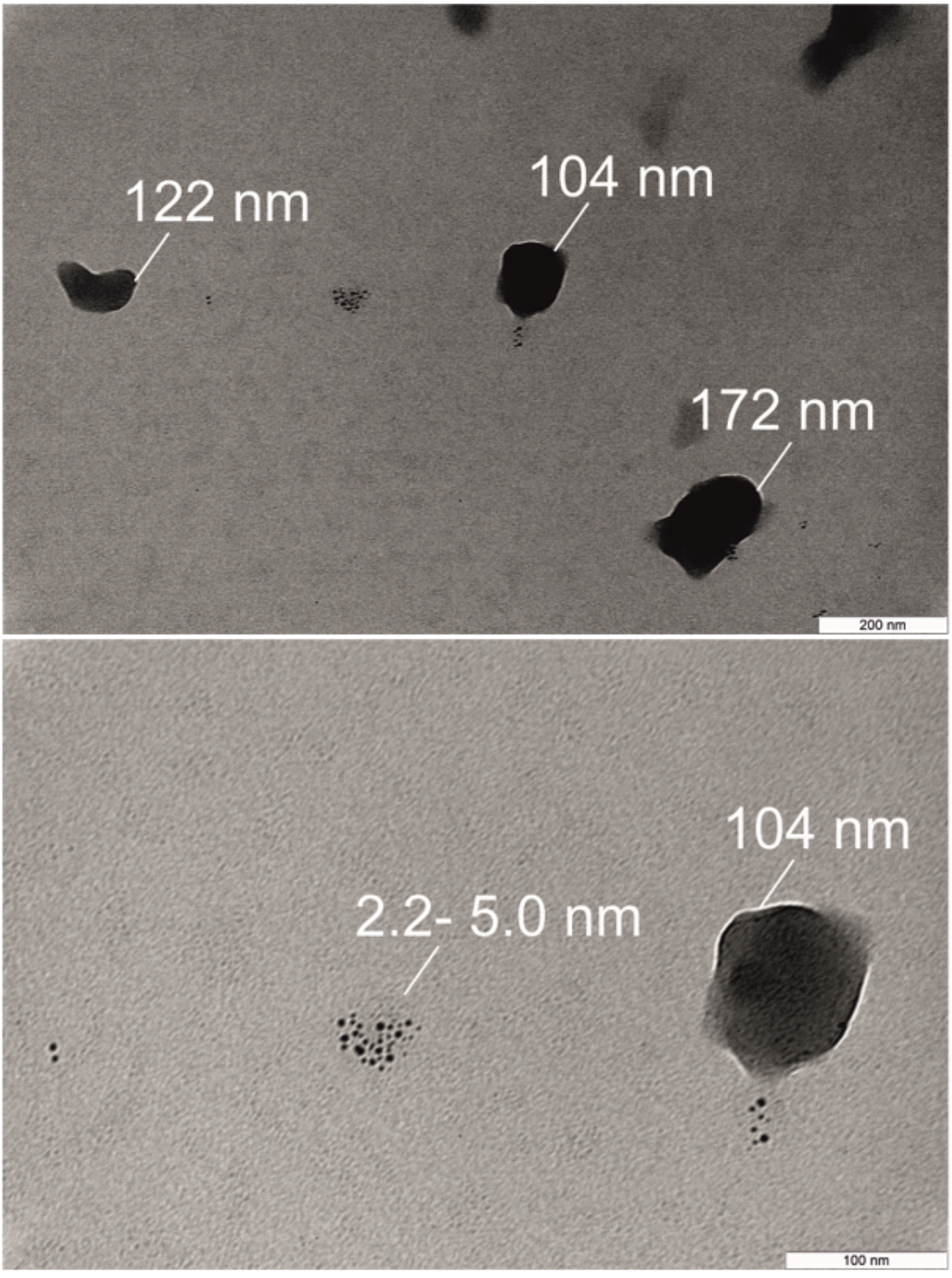

Figure 1

A, B. Nanoplastic particles in water and a plant's thallus. From left to right: a TEM image of a nanoplastic fragment and a magnified region of the fragment revealing smaller particles, demonstrating variation in particle size.

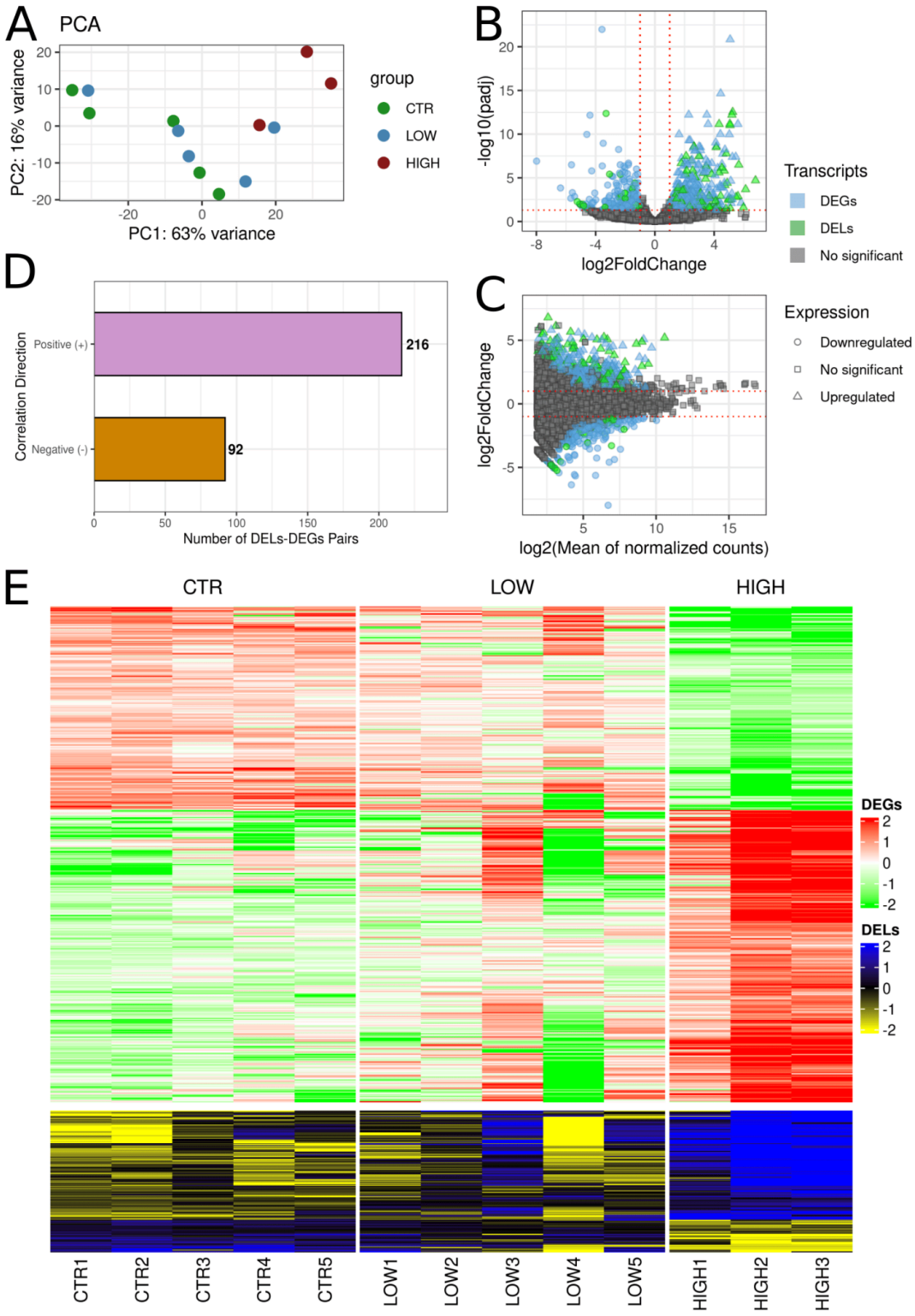

Figure 2

Quantitative analysis of expression profiling of *Riccia fluitans* tallus exposed on nano-/microplastic. A — A Principal Component Analysis (PCA) plot for all samples was constructed based on gene expression data . B — The volcano plot showing differentially expressed genes (DEGs, blue color) and differentially expressed long noncoding RNAs (DELs, green color). The x-axis represents logarithmic scale of expression fold change , while the y-axis represents logarithmic transformation of adjusted p-value.

Upregulated genes are signed as triangles and downregulated genes are signed as dots. Statistically non-significant genes were indicated in gray. C — The MA plot describing normalized expression of all expressed genes (X axis) and logarithmic fold change measure. D — Number of correlations between DEGs and DELs according to Spearman coefficient. E — The heatmap visualization of genes (DEGs and DELs) specific to high-dose of micro-/ nanoplastic (MNP). The middle panel of the heatmap also takes account the expression of these genes under low dose of MNP treatment.

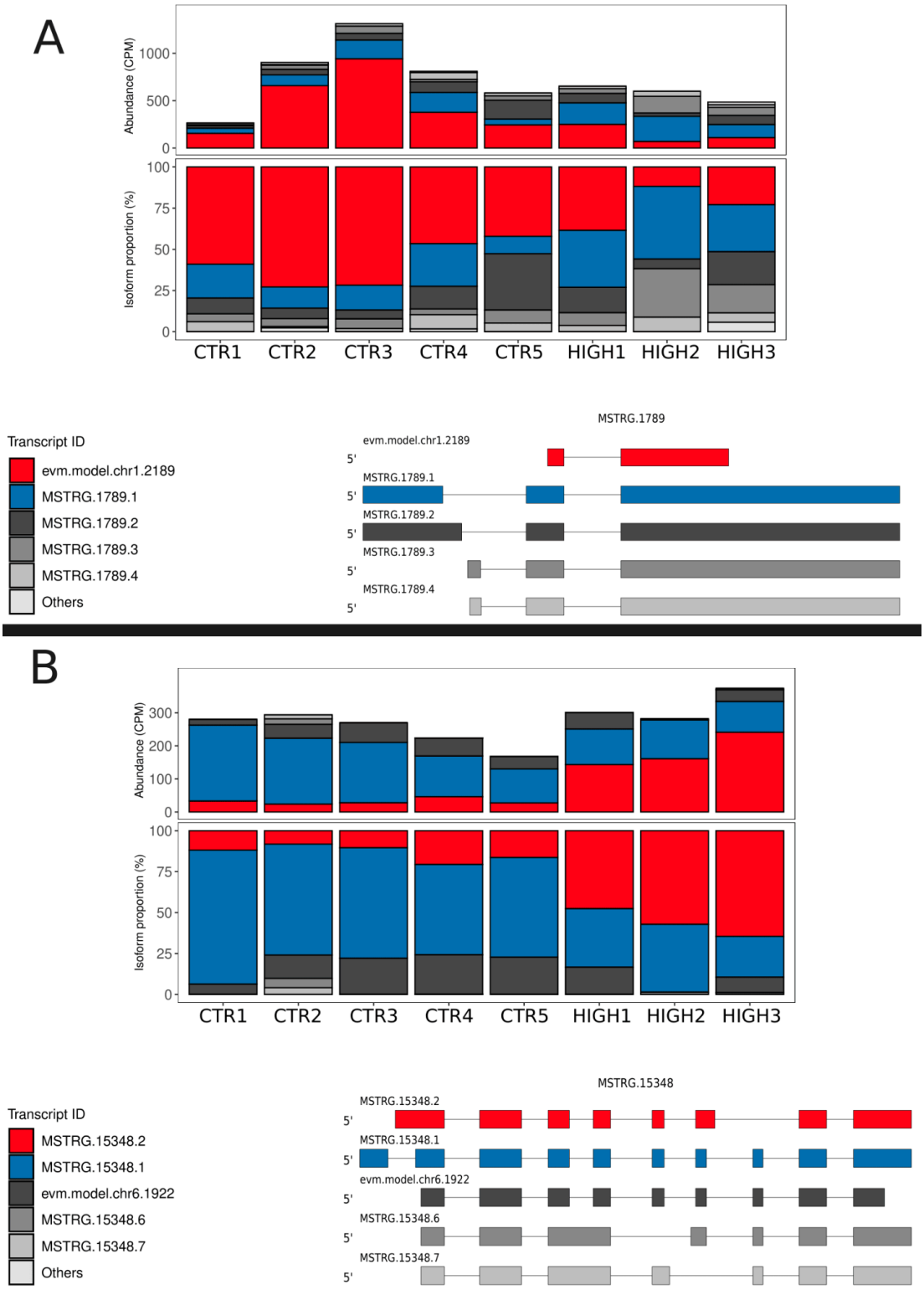

Figure 3

Difference in alternative splicing profiling of *Riccia fluitans* tallus exposed on nano-/microplastic. A — Alternative splicing modification within *CAL3* transcripts (A) and homologous sequences to *PAPR* transcripts (B), showing the proportions and CPM expression of transcripts in both conditions (CTR and high-dose of MNP) and gene structure of these gene targets. Red- and blue-colored transcripts differ significantly in the level of alternative splicing proportions between experimental conditions.

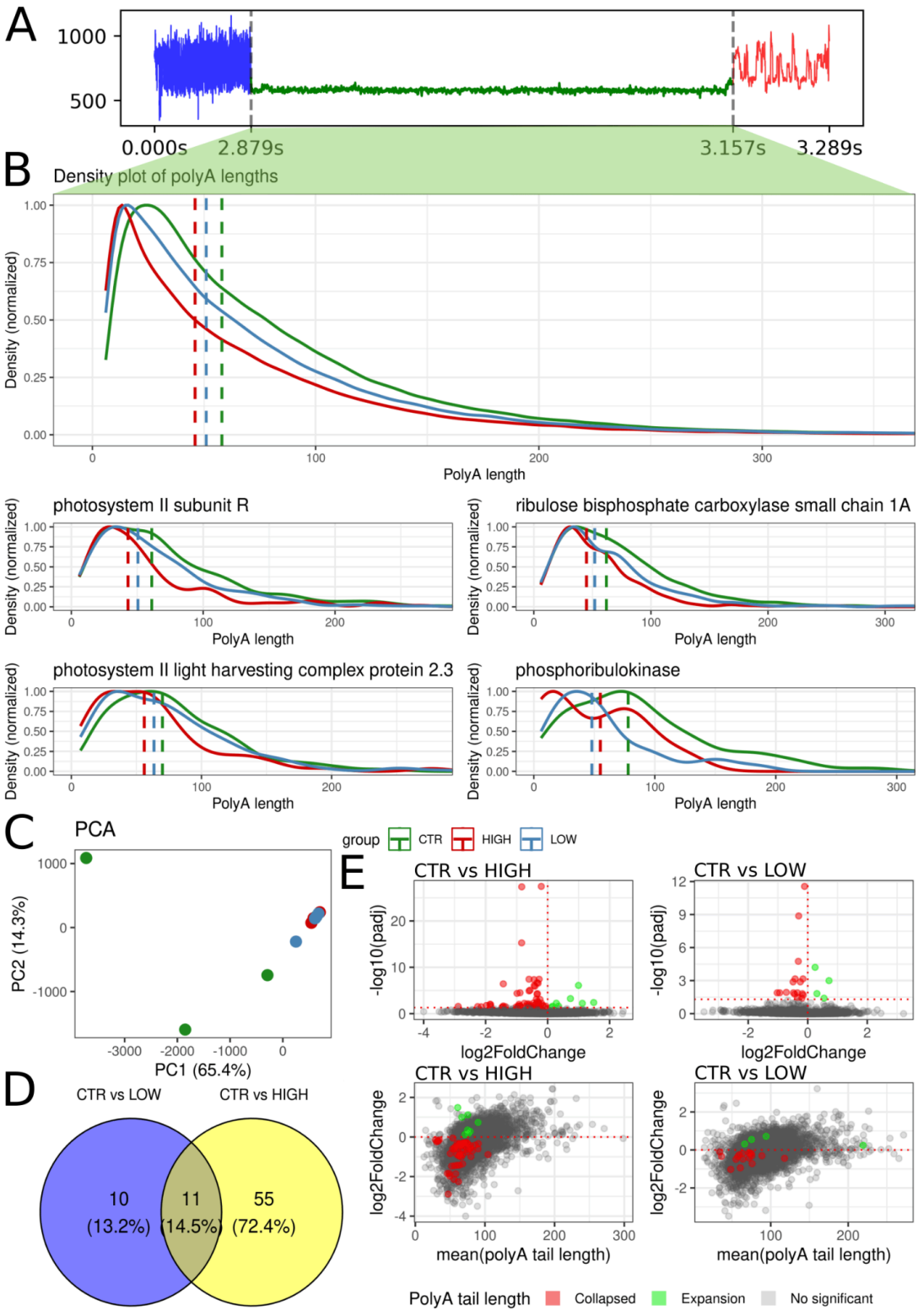

Figure 4

Quantitative analysis of polyA tail dynamics and differential polyadenylation patterns across nano-/microplastic exposure. A — An example of a raw nanopore sequencing signal is presented. The polyA tail is highlighted in green, the adapter is marked in red, and the transcript body is indicated in blue. B — Density plots of polyA tail lengths for the global dataset and selected genes are generated. The x-axis represents polyA tail length, while the y-axis represents normalized density. The CTR group is colored green, the HIGH group red, and the LOW group blue. Median values are symbolized by vertical dashed lines. C — A Principal Component Analysis (PCA) plot for all samples is constructed based on polyA tail length data. D — A Venn diagram is utilized to visualize unique and shared DPGs between the CTR vs. LOW (blue) and CTR vs. HIGH (yellow) comparisons. E — Volcano and MA plots are produced to characterize DPGs in the CTR vs. HIGH (left) and CTR vs. LOW (right) comparisons. DPGs categorized as 'Collapsed' are highlighted in red, while those identified as 'Expansion' are marked in green. Statistically non-significant genes are indicated in gray.

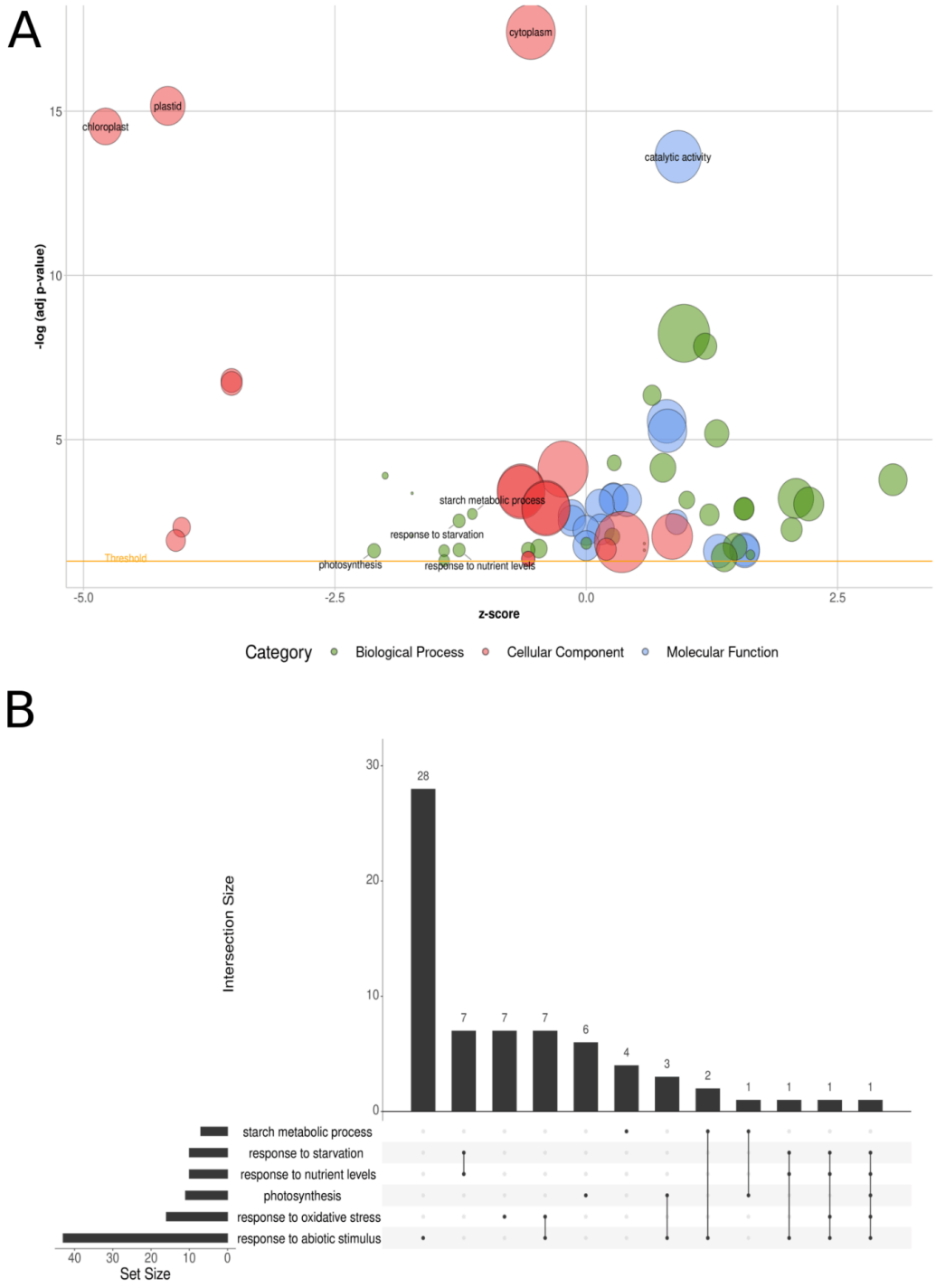

Figure 5

Gene ontology annotations of differentially expressed genes (DEGs) engaged in response to high-dose nano-/mikroplastic (MNP) treatment. Dot size describes the number of genes engaged in the GO term. Ontology terms are divided into three categories (A). The upset plot displays the selected GO terms that are modulated by MNP. Vertical bars represent the numbers of genes uniquely associated with individual processes (single dots) or the numbers of genes shared between two or more GO processes (dots

connected by lines). Horizontal bars indicate the total number of gene annotations for the six selected biological processes (B).

Analysis of GO processes and KEGG pathways enrichment (Table S7) revealed significant alterations in polyA length in plant response to low- and high-dose of nanoplastics. Particularly prominent were processes associated with photosynthesis and abiotic stress resistance. The most significantly enriched GO biological process term was "photosynthesis, light harvesting in photosystem I" (GO:0009768), involving five homologues of Arabidopsis thaliana: AT2G05100 - *LHCB2.1*, AT3G27690 - *LHCB2.3*, AT1G08380 - *PSAO*, AT2G05070 - *LHCB2.2*and AT1G61520 - *LHCA3*. The broader "photosynthesis" term (GO:0015979) encompassed 10 genes, including components of light reactions (GO:0019684). Molecular functions included GO terms such as "chlorophyll binding" (GO:0016168) and GO cellular component "thylakoid" (GO:0009579). The "photosynthesis" pathway (KEGG:00195) featured five genes such as AT1G60950 - *FD2*, AT1G76100 - *PETE1*, AT4G04640 - *ATPC1*, AT1G08380 - *PSAO* and AT1G79040 - *PSBR* (Fig. 6). The FD2 gene indicated modification on polyA tail length and also on gene expression profile under high-dose MNP treatment. Other GO terms related to "Response to stress" (GO:0006950) involved 19 genes, linked to "response to abiotic stimulus" (GO:0009628). ROS-related terms included "reactive oxygen species biosynthetic process" (GO:1903409) and "response to desiccation" (GO:0009269). No strongly enriched KEGG pathways specific to stress were identified ("Metabolic pathways" KEGG: 01100). These findings indicate nanoplastics-induced disruption of photosynthesis alongside activation of antioxidative mechanisms.

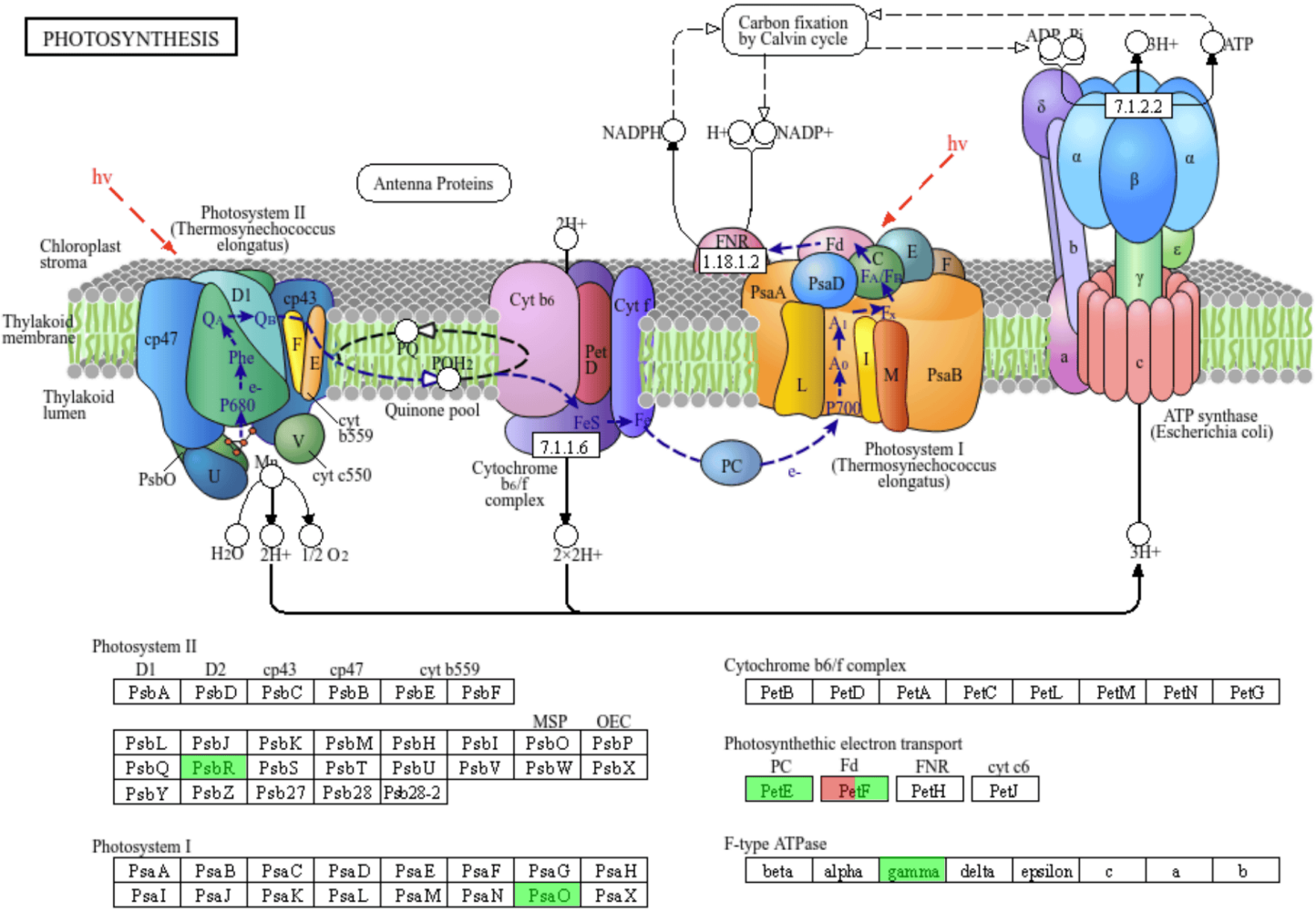

Figure 6

KEGG pathway enrichment annotation for photosynthesis with DEG candidates and genes with altered polyA tails. Red indicates a change in the overall expression profile, while green rectangles reveal modifications to poly A tails.

Supplementary Files

This is a list of supplementary files associated with this preprint. Click to download.

- SupplementaryTable.pdf